

# A third family of super dense stars in the presence of antikaon condensates

Sarmistha Banik and Debades Bandyopadhyay

*Saha Institute of Nuclear Physics, 1/AF Bidhannagar, Calcutta 700 064, India*

## Abstract

The formation of  $K^-$  and  $\bar{K}^0$  condensation in  $\beta$ -equilibrated hyperonic matter is investigated within a relativistic mean field model. In this model, baryon-baryon and (anti)kaon-baryon interactions are mediated by the exchange of mesons. It is found that antikaon condensation is not only sensitive to the equation of state but also to antikaon optical potential depth. For large values of antikaon optical potential depth,  $K^-$  condensation sets in before the appearance of negatively charged hyperons. We treat  $K^-$  condensation as a first order phase transition. The Gibbs criteria and global charge conservation laws are used to describe the mixed phase. Nucleons and  $\Lambda$  hyperons behave dynamically in the mixed phase. A second order phase transition to  $\bar{K}^0$  condensation occurs in the pure  $K^-$  condensed phase. Along with  $K^-$  condensation,  $\bar{K}^0$  condensation makes the equation of state softer thus resulting in smaller maximum mass stars compared with the case without any condensate. This equation of state also leads to a stable sequence of compact stars called the third family branch, beyond the neutron star branch. The compact stars in the third family branch have different compositions and smaller radii than that of the neutron star branch.

*PACS:* 26.60.+c, 21.65.+f, 97.60.Jd, 95.30.Cq

## I. INTRODUCTION

There is a growing interest to understand whether a stable sequence of compact stars could exist in nature beyond a neutron star branch. From observations, two families of compact stars - white dwarfs and neutron stars, are known to us. The physical reasons for stability in white dwarfs and neutron stars are different. In white dwarfs, it is the Fermi pressure of degenerate electrons that stabilizes the stars. After the white dwarf branch, there exists no stable star having central densities in the range  $10^9 - 10^{14} \text{ gm/cm}^3$  as is evident from the mass-radius relationship obtained by the Tolman-Oppenheimer-Volkoff (TOV) equations [1]. The stability is regained in the neutron star branch. In this case, the Fermi pressure of degenerate and interacting baryons is responsible for the stability of neutron stars. The question is what is next to a neutron star branch - again an unstable region followed by a stable configurations of super dense stars! If this picture is true, what could be the mechanism behind the stability of a possible third family of compact stars? Gerlach [2] first pointed out that a third family of compact stars could be a possibility. He

noted that a jump in the equation of state (EoS) or equivalently a large discontinuity in the speed of sound beyond the central density corresponding to the maximum neutron star mass might result in a stable family of super dense stars beyond the neutron star branch. However, Wheeler et al. showed that there was no stable compact stars beyond a neutron star branch for a smooth EoS [3].

Neutron stars are very useful laboratories to investigate the properties of dense matter [1,4]. At the core of a neutron star, the matter density could exceed by a few times normal nuclear matter density. Various exotic forms of matter such as hyperonic matter, quark-hadron mixed phase and Bose-Einstein condensation of strange particles may appear there. Earlier it was found that there might be kinks in the EoS because of the appearance of an exotic form of matter in the high density regime. Consequently there is a discontinuity in the speed of sound. This motivated various groups to explore whether physical processes like a first order phase transition from hadronic matter to quark matter or hadronic matter to hyperonic matter could give rise to an EoS leading to a third family of compact stars [5–8]. It was shown by various authors that a first order quark-hadron phase transition could produce an EoS such that the neutron star branch is terminated by the softening in the EoS due to the mixed phase and the third family of compact stars attained a pure quark phase in the core [5,6,8]. Similarly, a first order phase transition from hadronic matter to hyperonic matter led to stable solutions beyond the neutron star branch for certain parameters sets of hyperon-hyperon interactions [7]. It was demonstrated in those calculations that non-identical stars of same mass but distinctly different radii and compositions could exist because of partial overlapping mass regions of the neutron star branch and the third family branch. These pairs are known as "neutron star twins" [5,6].

Besides quark-hadron phase transition and the formation of hyperonic matter, Bose-Einstein condensation of antikaons may occur in the  $\beta$ -stable and charge neutral dense matter. This antikaon condensation could be a first or second order phase transition [9]. It was first demonstrated by Kaplan and Nelson [10] using a chiral  $SU(3)_L \times SU(3)_R$  Lagrangian that  $K^-$ -meson may undergo Bose-Einstein condensation in dense hadronic matter formed in heavy ion collisions. The strongly attractive  $K^-$ -nucleon interaction lowers the effective mass of  $K^-$  mesons in dense matter. Consequently, the in-medium energy of  $K^-$  mesons decreases and s-wave condensation sets in when the in-medium energy of  $K^-$  mesons equals to its chemical potential. Later, this chiral model was applied to the study of  $K^-$  condensation in the core of neutron stars [11–14]. Also, the traditional meson exchange picture where baryons and (anti)kaons interact through meson exchange, was extensively exploited to investigate antikaon condensation in dense matter relevant to (proto)neutron stars [9,15–20]. The onset of  $K^-$  condensation in neutron star matter depends on the nuclear equation of state and also on the depth of antikaon optical potential.

The threshold density of  $K^-$  condensation in nucleons-only star matter is 3-4 times normal nuclear matter density. The net effect of  $K^-$  mesons in the condensate in neutron star matter is to maintain charge neutrality replacing electrons and soften the EoS resulting in the reduction of maximum mass of the star [9,12,15–17,19,20]. In the presence of hyperons,  $K^-$  condensation was delayed to higher density. Recently, we have investigated the formation of  $\bar{K}^0$  condensation along with  $K^-$  condensation in dense nuclear and hyperonic matter relevant to (proto)neutron stars within Relativistic Mean Field (RMF) models [19,20]. It was found that the onset of  $\bar{K}^0$  condensation always occurred later than that of  $K^-$  condensation.

With the onset of  $\bar{K}^0$  condensation, abundances of neutrons and protons become equal in the high density matter [19,20]. In the presence of hyperons, the thresholds of  $K^-$  and  $\bar{K}^0$  condensation are shifted to higher densities. Along with  $K^-$  condensate,  $\bar{K}^0$  condensate makes the EoS much softer resulting in smaller maximum mass star compared to the case without any condensate.

In this paper we investigate the effects of antikaon condensation on the equation of state within a RMF model where baryons and (anti)kaons are interacting via meson exchanges. Also, we study the properties of the third family of compact stars with this EoS. The paper is organised in the following way. In section 2, we describe the RMF model of strong interactions and different phases of dense matter. In section 3, the parameters of the model are discussed. Results of our calculation and their relations to the third family of compact stars are explained in section 4. Section 5 deals with summary and conclusions.

## II. FORMALISM

In this calculation, we describe a first order phase transition from hadronic matter to the antikaon condensed phase in compact stars. We adopt a relativistic field theoretical model to describe the pure hadronic matter, pure antikaon condensed matter and the mixed phase. The constituents of matter -  $n, p, \Lambda, \Sigma^+, \Sigma^-, \Sigma^0, \Xi^-, \Xi^0$  of the baryon octet and electrons and muons, in the hadronic phase are to satisfy beta-equilibrium and local charge neutrality condition. The strong interaction between baryons is mediated by the exchange of scalar and vector mesons. The model is also extended to include hyperon- hyperon interaction through two additional hidden-strangeness mesons- scalar meson  $f_0(975)$  (denoted hereafter as  $\sigma^*$ ) and the vector meson  $\phi(1020)$  [17]. Therefore the Lagrangian density for the pure hadronic phase is given by

$$\begin{aligned} \mathcal{L}_B = & \sum_B \bar{\psi}_B (i\gamma_\mu \partial^\mu - m_B + g_{\sigma B} \sigma - g_{\omega B} \gamma_\mu \omega^\mu - g_{\rho B} \gamma_\mu \mathbf{t}_B \cdot \boldsymbol{\rho}^\mu) \psi_B \\ & + \frac{1}{2} (\partial_\mu \sigma \partial^\mu \sigma - m_\sigma^2 \sigma^2) - U(\sigma) \\ & - \frac{1}{4} \omega_{\mu\nu} \omega^{\mu\nu} + \frac{1}{2} m_\omega^2 \omega_\mu \omega^\mu - \frac{1}{4} \boldsymbol{\rho}_{\mu\nu} \cdot \boldsymbol{\rho}^{\mu\nu} + \frac{1}{2} m_\rho^2 \boldsymbol{\rho}_\mu \cdot \boldsymbol{\rho}^\mu + \mathcal{L}_{YY} . \end{aligned} \quad (1)$$

Here  $\psi_B$  denotes the Dirac spinor for baryon B with vacuum mass  $m_B$  and isospin operator  $\mathbf{t}_B$ . The scalar self-interaction term [21] is

$$U(\sigma) = \frac{1}{3} g_2 \sigma^3 + \frac{1}{4} g_3 \sigma^4 . \quad (2)$$

The Lagrangian density ( $\mathcal{L}_{YY}$ ) responsible for hyperon-hyperon interaction is given by,

$$\begin{aligned} \mathcal{L}_{YY} = & \sum_B \bar{\psi}_B (g_{\sigma^* B} \sigma^* - g_{\phi B} \gamma_\mu \phi^\mu) \psi_B \\ & + \frac{1}{2} (\partial_\mu \sigma^* \partial^\mu \sigma^* - m_{\sigma^*}^2 \sigma^{*2}) - \frac{1}{4} \phi_{\mu\nu} \phi^{\mu\nu} + \frac{1}{2} m_\phi^2 \phi_\mu \phi^\mu . \end{aligned} \quad (3)$$

At the interior of compact stars, the generalised  $\beta$ -decay processes may be written in the form  $B_1 \longrightarrow B_2 + l + \bar{\nu}_l$  and  $B_2 + l \longrightarrow B_1 + \nu_l$  where  $B_1$  and  $B_2$  are baryons and  $l$

is a lepton. These weak processes conserve baryon number and electric charge and are in chemical equilibrium. Therefore the generic equation for chemical equilibrium condition is

$$\mu_i = b_i \mu_n - q_i \mu_e , \quad (4)$$

where  $\mu_n$ ,  $\mu_e$  and  $\mu_i$  are respectively the chemical potentials of neutrons, electrons and  $i$ -th baryon with  $\mu_i = (k_{F_i}^2 + m_i^{*2})^{1/2} + g_{\omega i} \omega_0 + g_{\phi i} \phi_0 + I_{3i} g_{\rho i} \rho_{03}$  and  $b_i$  and  $q_i$  are baryon and electric charge of  $i$ -th baryon respectively. The above equation implies that there are two independent chemical potentials  $\mu_n$  and  $\mu_e$  corresponding to two conserved charges i.e. baryon number and electric charge. In neutron stars, electrons are converted to muons by  $e^- \rightarrow \mu^- + \bar{\nu}_\mu + \nu_e$  when the electron chemical potential becomes equal to the muon mass. Therefore, we have  $\mu_e = \mu_\mu$  in a neutron star. In the pure hadronic phase, the total charge density is

$$Q^h = \sum_B q_B n_B^h - n_e - n_\mu = 0 \quad (5)$$

where  $n_B^h$  is the number density of baryon B in the pure hadronic phase and  $n_e$  and  $n_\mu$  are charge densities of electrons and muons respectively.

Solving the equations of motion in the mean field approximation [22] along with effective baryon masses ( $m_i^*$ ) and equilibrium conditions we immediately compute the equation of state in the pure hadronic phase. The energy density ( $\varepsilon^h$ ) is related to the pressure ( $P^h$ ) in this phase through the Gibbs-Duhem relation

$$P^h = \sum_i \mu_i n_i - \varepsilon^h . \quad (6)$$

Here  $\mu_i$  and  $n_i$  are chemical potential and number density for  $i$ -th species.

The pure antikaon condensed phase is composed of baryons, leptons and antikaons. In this phase, the constituents of matter are in chemical equilibrium under weak interactions and maintain local charge neutrality. The baryon-baryon interaction in the pure condensed phase is described by the Lagrangian density as given by Eq. (1). Earlier it was shown that nucleons in the pure nuclear and antikaon condensed matter behaved differently because of their dynamical nature [9]. It was attributed to different mean fields which nucleons experienced in the pure phases. We adopt a relativistic field theoretical approach for the description of (anti)kaon-baryon interaction [9]. Here, baryon-baryon and (anti)kaon-baryon interactions are treated on the same footing. We also include  $\bar{K}^0$  condensation in this calculation and it occurs as a second order phase transition in the pure  $K^-$  condensed phase. The Lagrangian density for (anti)kaons in the minimal coupling scheme is,

$$\mathcal{L}_K = D_\mu^* \bar{K} D^\mu K - m_K^{*2} \bar{K} K , \quad (7)$$

where the covariant derivative  $D_\mu = \partial_\mu + i g_{\omega K} \omega_\mu + i g_{\phi K} \phi_\mu + i g_{\rho K} t_K \cdot \boldsymbol{\rho}_\mu$ . The isospin doublet for kaons is denoted by  $K \equiv (K^+, K^0)$  and that for antikaons is  $\bar{K} \equiv (K^-, \bar{K}^0)$ . The effective mass of (anti)kaons in this minimal coupling scheme is given by

$$m_K^* = m_K - g_{\sigma K} \sigma - g_{\sigma^* K} \sigma^* , \quad (8)$$

where  $m_K$  is the bare kaon mass. In the mean field approximation [22] adopted here, the meson fields are replaced by their expectation values. The mean meson fields are denoted

by  $\sigma$ ,  $\sigma^*$ ,  $\omega_0$ ,  $\phi_0$  and  $\rho_{03}$ . The dispersion relation representing the in-medium energies of  $\bar{K} \equiv (K^-, \bar{K}^0)$  for  $s$ -wave ( $\mathbf{k} = 0$ ) condensation is given by

$$\omega_{K^-, \bar{K}^0} = m_K^* - g_{\omega K} \omega_0 - g_{\phi K} \phi_0 \mp \frac{1}{2} g_{\rho K} \rho_{03} , \quad (9)$$

where the isospin projection  $I_{3\bar{K}} = \mp 1/2$  for the mesons  $K^-$  ( $-$  sign) and  $\bar{K}^0$  ( $+$  sign) are explicitly written in the expression. Since the  $\sigma$  and  $\omega$  fields generally increase with density and both the terms containing  $\sigma$  and  $\omega$  fields in Eq.(9) are attractive for antikaons, the in-medium energies of  $\bar{K}$  mesons decrease in nuclear medium. On the other hand, in nucleon-only matter  $\rho_{03} \equiv n_p - n_n$  ( $n_p$  and  $n_n$  are the proton and neutron densities) is negative; thus the  $\rho$ -meson field favors the formation of  $\bar{K}^0$  condensation over that of  $K^-$  condensation. In hyperonic matter, the repulsive  $\phi$  meson term may delay the onsets of antikaon condensation [17]. The in-medium energies of kaons  $K \equiv (K^+, K^0)$  are given by,

$$\omega_{K^+, K^0} = m_K^* + g_{\omega K} \omega_0 + g_{\phi K} \phi_0 \pm \frac{1}{2} g_{\rho K} \rho_{03} . \quad (10)$$

It is evident here that kaon condensation may be impossible in  $\beta$ -equilibrated matter because the  $\omega$ -meson term is repulsive for kaons and dominates over the attractive  $\sigma$ -meson term at higher densities. However, the attractive  $\phi$  meson term may decrease kaon energies in the presence of hyperons [17].

The meson field equations in the pure condensed phase are derived from Eqs. (1)-(3) and (7) as

$$m_\sigma^2 \sigma = -\frac{\partial U}{\partial \sigma} + \sum_B g_{\sigma B} n_B^{\bar{K}, S} + g_{\sigma K} \sum_{\bar{K}} n_{\bar{K}} , \quad (11)$$

$$m_\sigma^{*2} \sigma^* = \sum_B g_{\sigma^* B} n_B^{\bar{K}, S} + g_{\sigma^* K} \sum_{\bar{K}} n_{\bar{K}} , \quad (12)$$

$$m_\omega^2 \omega_0 = \sum_B g_{\omega B} n_B^{\bar{K}} - g_{\omega K} \sum_{\bar{K}} n_{\bar{K}} , \quad (13)$$

$$m_\phi^2 \phi_0 = \sum_B g_{\phi B} n_B^{\bar{K}} - g_{\phi K} \sum_{\bar{K}} n_{\bar{K}} , \quad (14)$$

$$m_\rho^2 \rho_{03} = \sum_B g_{\rho B} I_{3B} n_B^{\bar{K}} + g_{\rho K} \sum_{\bar{K}} I_{3\bar{K}} n_{\bar{K}} . \quad (15)$$

Here the scalar and number density of baryon  $B$  in the antikaon condensed phase are respectively

$$n_B^{\bar{K}, S} = \frac{2J_B + 1}{2\pi^2} \int_0^{k_{FB}} \frac{m_B^*}{(k^2 + m_B^{*2})^{1/2}} k^2 dk , \quad (16)$$

$$n_B^{\bar{K}} = (2J_B + 1) \frac{k_{FB}^3}{6\pi^2} , \quad (17)$$

with effective baryonic mass  $m_B^* = m_B - g_{\sigma B} \sigma - g_{\sigma^* B} \sigma^*$ , Fermi momentum  $k_{FB}$ , spin  $J_B$ , and isospin projection  $I_{3B}$ . Note that for  $s$ -wave  $\bar{K}$  condensation, the scalar and vector densities of antikaons are same and those are given by [9]

$$n_{K^-, \bar{K}^0} = 2 \left( \omega_{K^-, \bar{K}^0} + g_{\omega K} \omega_0 + g_{\phi K} \phi_0 \pm \frac{1}{2} g_{\rho K} \rho_{03} \right) \bar{K} K = 2m_K^* \bar{K} K . \quad (18)$$

The total energy density in the antikaon condensed matter has contributions from baryons, leptons and antikaons and is given by,

$$\begin{aligned} \varepsilon^{\bar{K}} = & \frac{1}{2} m_\sigma^2 \sigma^2 + \frac{1}{3} g_2 \sigma^3 + \frac{1}{4} g_3 \sigma^4 + \frac{1}{2} m_{\sigma^*}^2 \sigma^{*2} + \frac{1}{2} m_\omega^2 \omega_0^2 + \frac{1}{2} m_\phi^2 \phi_0^2 + \frac{1}{2} m_\rho^2 \rho_{03}^2 \\ & + \sum_B \frac{2J_B + 1}{2\pi^2} \int_0^{k_{FB}} (k^2 + m_B^{*2})^{1/2} k^2 dk + \sum_l \frac{1}{\pi^2} \int_0^{K_{Fl}} (k^2 + m_l^2)^{1/2} k^2 dk + \varepsilon_3, \end{aligned} \quad (19)$$

where  $l$  goes over electrons and muons and the energy density for antikaons is

$$\varepsilon_3 = m_K^* (n_{K^-} + n_{\bar{K}^0}). \quad (20)$$

Since antikaons form  $s$ -wave Bose condensates, they do not directly contribute to the pressure so that the pressure is due to baryons and leptons only

$$\begin{aligned} P^{\bar{K}} = & -\frac{1}{2} m_\sigma^2 \sigma^2 - \frac{1}{3} g_2 \sigma^3 - \frac{1}{4} g_3 \sigma^4 - \frac{1}{2} m_{\sigma^*}^2 \sigma^{*2} + \frac{1}{2} m_\omega^2 \omega_0^2 + \frac{1}{2} m_\phi^2 \phi_0^2 + \frac{1}{2} m_\rho^2 \rho_{03}^2 \\ & + \frac{1}{3} \sum_B \frac{2J_B + 1}{2\pi^2} \int_0^{k_{FB}} \frac{k^4 dk}{(k^2 + m_B^{*2})^{1/2}} + \frac{1}{3} \sum_l \frac{1}{\pi^2} \int_0^{K_{Fl}} \frac{k^4 dk}{(k^2 + m_l^2)^{1/2}} . \end{aligned} \quad (21)$$

The effect of antikaons in the pressure term is through the meson fields, which change due to the presence of additional antikaon source terms in the equations of motions in Eqs. (11)-(15). In the absence of those source terms for antikaons, we retain the equations of motion for meson fields in the pure hadronic phase.

With the onset of  $\bar{K}$  condensation, other strangeness changing processes may occur such as,  $N \rightleftharpoons N + \bar{K}$  and  $e^- \rightleftharpoons K^- + \nu_e$ , where  $N \equiv (n, p)$  and  $\bar{K} \equiv (K^-, \bar{K}^0)$  denote the isospin doublets for nucleons and antikaons, respectively. The requirement of chemical equilibrium yields

$$\mu_n - \mu_p = \mu_{K^-} = \mu_e , \quad (22)$$

$$\mu_{\bar{K}^0} = 0 , \quad (23)$$

where  $\mu_{K^-}$  and  $\mu_{\bar{K}^0}$  are respectively the chemical potentials of  $K^-$  and  $\bar{K}^0$ . The above conditions determine the onsets of antikaon condensations. When the effective energy of  $K^-$  meson ( $\omega_{K^-}$ ) equals to its chemical potential ( $\mu_{K^-}$ ) which, in turn, is equal to  $\mu_e$ , a  $K^-$  condensate is formed. Similarly,  $\bar{K}^0$  condensation is formed when its in-medium energy satisfies the condition  $\omega_{\bar{K}^0} = \mu_{\bar{K}^0} = 0$ .

The total charge density in the antikaon condensed phase is

$$Q^{\bar{K}} = \sum_B q_B n_B^{\bar{K}} - n_{\bar{K}^-} - n_e - n_\mu = 0 \quad (24)$$

Now we describe the mixed phase of hadronic matter and  $K^-$  condensed matter. In earlier works, the Maxwell construction was employed for a first order phase transition to antikaon condensation [12,16,19,20]. It was argued that the Maxwell construction was adequate for a system with only one conserved charge [9,23]. However, neutron star matter

has more than one conserved charge. As evident from the generic equation of  $\beta$ -equilibrium (Eq. (4)) there are two independent chemical potentials namely  $\mu_n$  and  $\mu_e$  connected to the conservation of baryon number and electric charge, respectively. Therefore, a Maxwell construction in this case will result in a discontinuity in one of the chemical potentials [9,23]. It was shown by Glendenning [9,23] that the Gibbs conditions for thermodynamic equilibrium along with global conservation laws would be required to describe the mixed phase. For compact star matter the Gibbs phase rules read,

$$P^h = P^{\bar{K}}, \quad (25)$$

$$\mu_B^h = \mu_B^{\bar{K}}. \quad (26)$$

where  $\mu_B^h$  and  $\mu_B^{\bar{K}}$  are chemical potentials of baryon B in the pure hadronic and  $K^-$  condensed phase, respectively. The conditions of global charge neutrality and baryon number conservation are imposed through the relations

$$(1 - \chi)Q^h + \chi Q^{\bar{K}} = 0, \quad (27)$$

$$n_B = (1 - \chi)n_B^h + \chi n_B^{\bar{K}}, \quad (28)$$

where  $\chi$  is the volume fraction of  $K^-$  condensed phase in the mixed phase. The total energy density in the mixed phase is

$$\epsilon = (1 - \chi)\epsilon^h + \chi\epsilon^{\bar{K}}. \quad (29)$$

### III. PARAMETERS

In the effective field theoretic approach discussed here, knowledge of three distinct sets of coupling constants for nucleons, kaons and hyperons associated with the exchange of scalar  $\sigma$ , isoscalar-vector  $\omega$ , and vector-isovector  $\rho$  mesons and two additional hidden-strangeness mesons, scalar meson ( $\sigma^*$ ) and vector meson  $\phi$  are required. The nucleon-meson coupling constants generated by reproducing the nuclear matter saturation properties are taken from Glendenning and Moszkowski of Ref. [24]. This set is referred to as GM1 and its parameters are also listed in Table I.

The vector coupling constants for hyperons are determined from SU(6) symmetry as,

$$\begin{aligned} \frac{1}{2}g_{\omega\Lambda} &= \frac{1}{2}g_{\omega\Sigma} = g_{\omega\Xi} = \frac{1}{3}g_{\omega N}, \\ \frac{1}{2}g_{\rho\Sigma} &= g_{\rho\Xi} = g_{\rho N}; \quad g_{\rho\Lambda} = 0, \\ 2g_{\phi\Lambda} &= 2g_{\phi\Sigma} = g_{\phi\Xi} = -\frac{2\sqrt{2}}{3}g_{\omega N}. \end{aligned} \quad (30)$$

The scalar meson ( $\sigma$ ) coupling to hyperons is obtained from the potential depth of a hyperon (Y) in the saturated nuclear matter

$$U_Y^N(n_0) = -g_{\sigma Y}\sigma + g_{\omega Y}\omega_0. \quad (31)$$

The analysis of energy levels in  $\Lambda$ -hypernuclei suggests a well depth of  $\Lambda$  in symmetric nuclear matter  $U_{\Lambda}^N(n_0) = -30$  MeV [25,26]. On the other hand, recent analysis of a few  $\Xi$ -hypernuclei events in emulsion experiments predicts a  $\Xi$  well depth of  $U_{\Xi}^N(n_0) = -18$  MeV [27,28] in normal nuclear matter. However, the situation for the  $\Sigma$  potential depth in normal nuclear matter is very unclear. The only known bound  $\Sigma$ -hypernucleus is  ${}^4_{\Sigma}He$  [29]. The most updated analysis of  $\Sigma^-$  atomic data indicates a strong isoscalar repulsion in  $\Sigma$ -nuclear matter interaction [30]. Therefore, we use a repulsive  $\Sigma$  well depth of  $U_{\Sigma}^N(n_0) = 30$  MeV [30] in this calculation.

The  $\sigma^*$ -Y coupling constants are obtained by fitting them to a well depth,  $U_Y^{(Y')}(n_0)$ , for a hyperon (Y) in a hyperon ( $Y'$ ) matter at nuclear saturation density [17,31]. It is given as

$$U_{\Xi}^{(\Xi)}(n_0) = U_{\Lambda}^{(\Xi)}(n_0) = 2U_{\Xi}^{(\Lambda)}(n_0) = 2U_{\Lambda}^{(\Lambda)}(n_0) = -40 \quad (32)$$

Nucleons do not couple to the strange mesons i.e.  $g_{\sigma^*N} = g_{\phi N} = 0$ .

Now we determine kaon-meson coupling constants. According to the quark model and isospin counting rule, the vector coupling constants are given by

$$g_{\omega K} = \frac{1}{3}g_{\omega N} \quad \text{and} \quad g_{\rho K} = g_{\rho N} . \quad (33)$$

The scalar coupling constant is obtained from the real part of  $K^-$  optical potential depth at normal nuclear matter density

$$U_{\bar{K}}(n_0) = -g_{\sigma K}\sigma - g_{\omega K}\omega_0 . \quad (34)$$

The strange meson fields also couple with (anti)kaons. Following Ref.[ [17]], the  $\sigma^*$ -K coupling constant is determined from the decay of  $f_0(925)$  as  $g_{\sigma^*K} = 2.65$ , whereas the vector  $\phi$  meson coupling with (anti)kaons is obtained from SU(3) relation as  $\sqrt{2}g_{\phi K} = 6.04$ .

It was observed in previous calculations that antikaons experienced an attractive potential and kaons had a repulsive interaction in nuclear matter [30,32–36]. The analysis of  $K^-$  atomic data in the hybrid model [32] yielded the real part of the antikaon optical potential as large as  $U_{\bar{K}} = -180 \pm 20$  MeV at normal nuclear matter density but it was repulsive at low density in accordance with the low density theorem. Also, the antikaon potential depth in the coupled channel calculation [33] was found to be  $U_{\bar{K}} = -100$  MeV whereas the chirally motivated coupled channel approach [34] gave rise to a potential depth of  $U_{\bar{K}} = -120$  MeV. The different treatments of  $\Lambda(1405)$  resonance which is considered to be an unstable  $\bar{K}N$  bound state just below  $K^-p$  threshold, may be responsible for the wide range of antikaon optical potential depth values in various calculations. In Table II, we list kaon- $\sigma$  meson coupling constant  $g_{\sigma K}$ , for a set of antikaon optical potential depths starting from -100 MeV to -180 MeV.

#### IV. RESULTS AND DISCUSSION

The conversion of nucleons to hyperons is energetically favorable in  $\beta$ - equilibrated and charge neutral dense matter. Hyperons first appear in dense matter around  $(2-3)n_0$ . Negatively charged hyperons quench the growth of electron chemical potential. Also the equation of state is softened in the presence of hyperons. Therefore, it was shown in various

calculations neglecting hyperon-hyperon interaction that the formation of  $\bar{K}$  condensate was postponed to higher densities [13,16,19,20]. As the matter is hyperon-rich in the high density regime, hyperon-hyperon interaction becomes important. This interaction may be accounted by including two additional mesons  $\sigma^*$  and  $\phi$ . These strange mesons also couple with (anti)kaons. It follows from strangeness numbers of hyperons and  $\bar{K}$  mesons that the  $\phi$  field is repulsive for hyperons as well as for antikaons. The additional attraction due to  $\sigma^*$  field makes the EoS softer. On the other hand, the repulsive contribution of  $\phi$  field becomes dominant at higher densities and a stiffer EoS is obtained. For calculations with GM1 set and various values of  $|U_{\bar{K}}(n_0)| < 160$  MeV, we find that the threshold of  $K^-$  condensation in  $\beta$ -equilibrated hyperonic matter is shifted to very high density ( $7.5n_0$ ) where effective nucleon mass becomes small [19,20]. This is attributed to the early appearance of  $\Xi^-$  hyperons which diminish the electron chemical potential and the presence of repulsive  $\phi$  field in the expression of energy for  $K^-$  and  $\bar{K}^0$  mesons (Eq.(9)).

Now we perform our calculation using GM1 set and antikaon optical potential depth of  $U_{\bar{K}}(n_0) = -160$  MeV. In Figure 1 we exhibit the particle fraction of  $\beta$ -equilibrated matter containing baryons, electrons, muons and  $K^-$  mesons. In the pure hadronic phase where local charge neutrality condition is imposed, abundances of nucleons, electrons and muons increase with density. Here, charge neutrality is maintained among protons, electrons and muons. With the onset of  $K^-$  condensation, the mixed phase begins at  $2.23n_0$ . This mixed phase is determined by the Gibbs phase rules for pure hadronic and antikaon condensed phase in thermodynamic equilibrium and by global baryon number and electric charge conservation laws. We find that  $\Lambda$  hyperon is the first strange baryon to appear in the mixed phase at  $2.51n_0$ . The total baryon density in the mixed phase is the sum of two contributions from the hadronic and antikaon condensed phase weighted with appropriate volume fractions. As soon as  $K^-$  condensate is formed, it rapidly grows with density and replaces electrons and muons. Being bosons,  $K^-$  mesons in the lowest energy state are energetically more favorable to maintain charge neutrality than any other negatively charged particles. Consequently, the proton density becomes equal to the density of  $K^-$  condensate. Also, the density of  $\Lambda$  hyperon increases with density in the mixed phase. On the other hand, the neutron density decreases in the mixed phase. The reason behind it may be the creation of more protons in the presence of  $K^-$  condensate and also the growth of  $\Lambda$  hyperons at the expense of neutrons. The mixed phase terminates at  $4.0n_0$ . Heavier hyperons appear in the pure condensed phase. As  $\Xi^-$  hyperons start populating this phase at  $6.77n_0$ , the density of  $K^-$  condensate falls. However, the rising behavior of  $K^-$  condensate is regained with the onset of  $\Sigma^+$  hyperons at  $7.86n_0$ . It is to be noted that  $\Sigma^-$  hyperons do not appear in this case.

Besides  $K^-$  condensation, we now investigate the role of  $\bar{K}^0$  condensation in  $\beta$ -equilibrated and charge neutral matter consisting of nucleons, hyperons, electrons and muons. The abundances of various species are shown in Figure 2. The composition of the pure hadronic and mixed phase in this case is similar to that of Fig. 1. Once the mixed phase is over,  $\bar{K}^0$  condensation occurs at  $\sim 4.1n_0$ . We consider  $\bar{K}^0$  condensation as a second order phase transition. The antikaon condensed phase including  $\bar{K}^0$  condensate along with  $K^-$  condensate is different from that of Fig. 1. With the appearance of  $\bar{K}^0$  condensate, neutron and proton abundances become equal and a symmetric matter of nucleons is formed in this phase. The density of  $\bar{K}^0$  condensate increases with baryon density uninterruptedly and even becomes larger than the density of  $K^-$  condensate. At higher densities, more

hyperons start populating the system. As soon as negatively charged hyperons -  $\Xi^-$  and  $\Sigma^-$  appear, the density of  $K^-$  condensate is observed to fall drastically. This is quite expected because it is energetically favorable for particles carrying conserved baryon numbers to achieve charge neutrality in the system. Leptons or mesons are no longer required for this sole purpose. Moreover, lepton number or meson number is not conserved in the star. The system is dominated by  $\bar{K}^0$  condensate in the high density regime.

One important aspect of this calculation is the dynamic behavior of baryons in pure hadronic and antikaon condensed phase. Earlier, this dynamical behavior of nucleons was noted by Glendenning and Schaffner [9]. Besides nucleons, we find similar properties of  $\Lambda$  hyperons which appear in the mixed phase. It is evident from Eq. (11) and Eq. (12) that baryons have different effective masses in the hadronic and condensed phase due to different  $\sigma$  and  $\sigma^*$  fields. In the pure hadronic phase, the effective mass of a baryon decreases with density. With the onset of the mixed phase, a second solution for the effective baryon mass emerges. This is the effective baryon mass in the condensed phase. The value of the effective baryon mass in the pure hadronic phase is always higher than that of the antikaon condensed phase. In the condensed phase, the effective mass of a baryon also decreases with density.

Equation of state, pressure(P) versus energy density ( $\varepsilon$ ), for  $\beta$ -equilibrated and charge neutral matter with different compositions are displayed in Figure 3. Here the long-dashed curve stands for hyperonic matter without any antikaon condensate. The dotted curve represents hyperonic matter including  $K^-$  condensate whereas the solid curve corresponds to hyperonic matter with both  $K^-$  and  $\bar{K}^0$  condensate. The EoS denoted by the dashed-dot curve is same as given by the solid except no  $\Xi$  hyperon is present in the system in this case. Two kinks in the solid curve marks the beginning and end of the mixed phase where pure hadronic and  $K^-$  condensed phase are in thermodynamic equilibrium as dictated by the Gibbs conditions and global conservation laws. Immediately after the termination of the mixed phase at  $4.0n_0$ ,  $\bar{K}^0$  condensation sets in at  $\sim 4.1n_0$ . We have treated here  $\bar{K}^0$  condensation as a second order phase transition. Also we find that the pressure increases continuously with energy (solid curve) after the formation of  $\bar{K}^0$  condensation. Earlier it was noted that the antikaon condensation could be a second order phase transition depending on the strength of antikaon optical potential depth and parameter sets of different models [9,19,20]. Though the dotted curve has overlap with the solid curve up to the mixed phase, it becomes stiffer in the high density regime. On the other hand, the dashed-dot curve becomes stiffer compared to the solid curve because there is lesser number of degrees of freedom with the absence of  $\Xi$  hyperons in the former case. With the appearance of both  $K^-$  and  $\bar{K}^0$  condensation in hyperonic matter, the overall EoS (solid curve) is softened due to the strong attraction imparted by antikaon condensation.

We have used the results of Baym, Pethick and Sutherland [37] to describe the crust of a compact star composed of leptons and nuclei for the low density ( $n_B < 0.001 fm^{-3}$ ) EoS. In the mid density regime ( $0.001 \leq n_B < 0.08 fm^{-3}$ ) the results of Negele and Vautherin [38] are taken into account. Above this density, an EoS calculated in the relativistic model has been adopted.

Now we present the results of static structures of spherically symmetric compact stars calculated using TOV equations. The static compact star sequences representing the stellar masses  $M/M_\odot$  and the corresponding central energy densities  $\varepsilon_c$  are shown in Figure 4. We denote the sequence of neutron stars with  $K^-$  condensation in hyperonic matter by

the dotted curve. Here, the maximum neutron star mass is  $1.649M_{\odot}$  occurring at central density  $7.7n_0$ . The maximum neutron star mass consisting only of hyperons is  $1.789M_{\odot}$  corresponding to the central density  $5.16n_0$  (not shown in the Figure). The solid curve represents compact stars with both  $K^-$  and  $\bar{K}^0$  condensation in hyperonic matter. When  $\bar{K}^0$  condensation along with  $K^-$  condensation is taken into account, the limiting mass of the neutron star branch is attained at much earlier central density  $4.49n_0$ . In fact, the limiting mass star appears very close to the upper boundary of the mixed phase and has a smaller value  $1.571M_{\odot}$  than the situation with only  $K^-$  condensation. This reduction in the maximum mass of the star may be attributed to the softening of the EoS in the presence of  $K^-$  and  $\bar{K}$  condensate. After the stable neutron star branch, there is an unstable region followed by a sequence of compact stars in Fig. 4. This branch of super dense stars beyond the neutron star branch is called a third family of compact stars [2,5,6]. There are two third family branches in Fig. 4. The lower curve depicts the third family of compact stars with both antikaon condensates in hyperonic matter (case I) whereas the upper curve represents the third family of compact stars including both condensates in hyperonic matter except  $\Xi$  hyperons (case II). The maximum masses of compact stars in the third family branches denoted by the lower curve and upper curve are  $1.552M_{\odot}$  and  $1.561M_{\odot}$  corresponding to the central densities  $8.09n_0$  and  $9.20n_0$  respectively. It is the behavior of the EoS including both  $K^-$  and  $\bar{K}^0$  condensate in the mid and high density regime that results in a third family of super dense star. The possibility of a third family of compact stars was already discussed in the context of quark-hadron phase transition [5,6] and hadronic matter to hyperonic matter phase transition [7].

We have found a new sequence of compact stars called the third family of compact stars beyond the neutron star branch as is evident in Fig. 4. So far, we have discussed the hydrostatic stability of the stellar sequence in the third family using TOV equations [1]. In Fig. 4, we note that the neutron star branch or the third family branch has positive slope i.e.  $dM/d\varepsilon_c > 0$ . Though the positive slope of a stellar sequence is a necessary condition for stability, dynamical stability requires the analysis of the fundamental mode of radial vibration [5,6,39–41]. In the third family branches in Fig. 4, we find that each configuration is stable because the squared frequency of the fundamental mode associated with it is positive. Similar results were obtained in the study of compact stars beyond the neutron star branch using quark-hadron phase transition by various groups [5,6].

We exhibit the mass-radius relationship for different EoS in Figure 5. The maximum mass star composed of hyperons and no condensate (not shown here) has a radius of 12.8 Km whereas it is 10.9 Km for the maximum mass neutron star including hyperons and  $K^-$  condensate (dotted curve). Two cases where we obtain stable solutions beyond the neutron star branch are shown in the inset. The solid curve denotes the sequences of compact stars having hyperons and  $K^-$  and  $\bar{K}^0$  condensate. In the neutron star branch, the maximum mass star has a radius of 12.8 Km. For the third family branches, the lower curve corresponds to case I and the upper curve denotes case II. The radius of the maximum mass super dense star on the lower curve is 10.7 Km whereas that of case II is 10.2 Km. In this calculation, we find that the existence of non-identical stars of same mass may be possible because of partial overlapping of the neutron star and the third family branch. These pairs are known as "neutron star twins" [5,6]. Also, we observe that the high density twin is a very compact object with a different composition and smaller radius than its low density counter part. It

is to be noted that the radius of the maximum mass star with  $K^-$  condensate in hyperonic matter is comparable to that of the third family considered here. This implies that only one star with small radius cannot ensure the existence of a third family of compact stars. Schertler et al. [6] argued that two stars - one in the neutron star branch and the other in the third family branch with similar masses but with a radius difference of a few kilometer might reveal the existence of a third family of compact stars. In this case, the mass difference ( $\Delta M$ ) of two stars is to be much less than the radius difference ( $\Delta R$ ) i.e.  $\Delta M \ll \Delta R$ . In our calculation, we note that  $\Delta R$  is almost two orders of magnitude larger than  $\Delta M$ .

We also investigate the high density behaviour of the equation of state in TM1 model [42]. Besides scalar self interaction terms, TM1 model includes non-linear  $\omega$  meson term [42,43]. The parameters of TM1 model are listed in Table I and Table II. In this model, antikaon condensations are found to be second order phase transitions for all values of antikaon optical potential depth [9,19,20]. The EoS behaves smoothly even in the high density regime. There is no existence of a third family of compact stars in TM1 model because of this smooth EoS.

## V. SUMMARY AND CONCLUSIONS

We have investigated  $K^-$  and  $\bar{K}^0$ -meson condensation in  $\beta$ -equilibrated hyperonic matter within a relativistic mean field model. In this model, baryon-baryon and (anti)kaon-baryon interactions are mediated by the exchange of  $\sigma$ ,  $\omega$  and  $\rho$  meson. Also, hyperon-hyperon interaction is accounted by considering two additional strange mesons  $\sigma^*$  and  $\phi$ . In this calculation, we have adopted GM1 parameter set. The coupling constants of (anti)kaon-meson are determined from a quark model and empirically known values of antikaon optical potential depth at normal nuclear matter density. Similarly, the hyperon-meson coupling constants are obtained from hypernuclear data and SU(6) symmetry relations. However, the coupling constant of hyperons to  $\sigma^*$  meson is obtained by reproducing the hyperon depth in a bath of the hyperons at normal nuclear matter density.

The condensation of  $K^-$  meson in hyperonic matter is described as a first order phase transition in this calculation. The  $\beta$ -equilibrated matter is composed of three phases - pure hadronic phase, pure  $K^-$  condensed phase and the mixed phase of two pure phases. Along with the Gibbs phase rules, global conservation laws are employed in the mixed phase.

The appearance of antikaon condensation is quite sensitive to the EoS and also depends on the value of antikaon optical potential depth. In the presence of hyperons, an EoS becomes softer thus delaying the onset of antikaon condensation. For antikaon optical potential depth  $|U_{\bar{K}}(n_0)| < 160$  MeV, the early appearance of negatively charged hyperons in particular  $\Xi^-$  hyperons, reduces the electron chemical potential. And the antikaon condensation does not occur even at  $7.5n_0$ . In our calculation with  $U_{\bar{K}}(n_0) = -160$  MeV, the first order phase transition to  $K^-$  condensation begins at  $4.0n_0$ . The pure hadronic phase does not contain any hyperon whereas only  $\Lambda$  hyperons appear in the mixed phase. As soon as  $K^-$  condensation sets in, it is energetically favourable for  $K^-$  mesons in the zero momentum state to maintain charge neutrality in the system. Consequently, the formation of negatively charged hyperons are delayed to higher density. Immediately after the end of the mixed phase,  $\bar{K}^0$  condensation occurs in the pure  $K^-$  condensed phase. Here, we have treated  $\bar{K}^0$  condensation as a second order phase transition. With the formation of  $\bar{K}^0$  condensation, abundances of neutron and protons become equal. Negatively charged hyperons -  $\Xi^-$  and

$\Sigma^-$  start populating the system around  $\sim 7n_0$ . And the density of  $K^-$  condensate dwindles because hyperons having conserved baryon number are energetically more favourable for charge neutrality. Consequently,  $\bar{K}^0$  condensate dominates the high density regime.

The equation of state becomes softer in the presence of antikaon condensate compared with the situation without any condensate. Among all EoS considered here, the softest EoS is the one that includes both  $K^-$  and  $\bar{K}^0$  condensate. This softening leads to the reduction in maximum masses of compact stars. The behaviour of the EoS with both antikaon condensates at very high density  $\sim 8 - 10n_0$  and its connection to the possible existence of stable super dense stars beyond the neutron star branch have been investigated in this work. With the EoS corresponding to hyperonic matter with  $K^-$  and  $\bar{K}^0$  condensate, we find, after the termination of the neutron star branch, an unstable region followed by a stable sequence of compact stars called the third family of compact stars. It is noted that neutron star twins could exist because of partially overlapping mass regions of the neutron star branch and the third family branch. The high density twin in the third family branch has a different composition and smaller radius than its low density counter part. The observation of two compact stars with almost similar masses but different radii may shed light on the existence of a third family of super dense stars.

## REFERENCES

- [1] N.K. Glendenning, *Compact Stars* (Springer-Verlag, New York, 1997).
- [2] U.H. Gerlach, *Physical Review* **172**, 1325 (1968).
- [3] B.K. Harrison, K.S. Thorne, M. Wakano and J.A. Wheeler, *Gravitation Theory and Gravitational Collapse*, (University of Chicago Press, Chicago, 1965).
- [4] F. Weber, *Pulsars as Astrophysical Laboratories for Nuclear and Particle Physics* (IOP Publishing, Bristol, 1998).
- [5] N.K. Glendenning and C. Kettner, *Astron. Astrophys.* **353**, L9 (2000).
- [6] K. Schertler, C. Greiner, J. Schaffner-Bielich and M.H. Thoma, *Nucl. Phys.* **A677**, 463 (2000).
- [7] J. Schaffner-Bielich, M. Hanauske, H. Stöcker and W. Greiner, astro-ph/0005490.
- [8] E.S. Fraga, R.D. Pisarski and J. Schaffner-Bielich, *D* **63**, 121702 (2001).
- [9] N.K. Glendenning and J. Schaffner-Bielich, *Phys. Rev. C* **60**, 025803 (1999).
- [10] D.B. Kaplan and A.E. Nelson, *Phys. Lett. B* **175**, 57 (1986);  
A.E. Nelson and D.B. Kaplan, *Phys. Lett. B* **192**, 193 (1987).
- [11] G.E. Brown, K. Kubodera, M. Rho and V. Thorsson, *Phys. Lett. B* **291**, 355 (1992).
- [12] V. Thorsson, M. Prakash and J.M. Lattimer, *Nucl. Phys.* **A572**, 693 (1994).
- [13] P.J. Ellis, R. Knorren and M. Prakash, *Phys. Lett. B* **349**, 11 (1995).
- [14] M. Prakash, I. Bombaci, M. Prakash, P.J. Ellis, J.M. Lattimer and R. Knorren, *Phys. Rep.* **280**, 1 (1997).
- [15] T. Muto, *Prog. Theo. Phys.* **89**, 415 (1993).
- [16] R. Knorren, M. Prakash and P.J. Ellis, *Phys. Rev. C* **52**, 3470 (1995).
- [17] J. Schaffner and I.N. Mishustin, *Phys. Rev. C* **53**, 1416 (1996).
- [18] J.A. Pons, S. Reddy, P.J. Ellis, M. Prakash, and J.M. Lattimer, *Phys. Rev. C* **62** 035803 (2000).
- [19] S. Pal, D. Bandyopadhyay and W. Greiner, *Nucl. Phys.* **A674**, 553 (2000).
- [20] S. Banik and D. Bandyopadhyay, *Phys. Rev. C* **63**, 035802 (2001).
- [21] J. Boguta and A.R. Bodmer, *Nucl. Phys.* **A292**, 413 (1977).
- [22] B.D. Serot and J.D. Walecka, *Adv. in Nucl. Phys.* **16**, 1 (1986).
- [23] N.K. Glendenning, *Phys. Rev. D* **46**, 1274 (1992).
- [24] N.K. Glendenning and S.A. Moszkowski, *Phys. Rev. Lett.* **67**, 2414 (1991).
- [25] R.E. Chrien and C.B. Dover, *Annu. Rev. Nucl. Part. Sci.* **39**, 113 (1989).
- [26] C.B. Dover and A. Gal, *Prog. Part. Nucl. Phys* **12**, 171 (1984).
- [27] T. Fakuda et al., *Phys. Rev. C* **58**, 1306 (1998).
- [28] P. Khaustov et al., *Phys. Rev. C* **61**, 054603 (2000).
- [29] R.S. Hayano et al., *Phys. Lett. B* **231**, 355 (1989).
- [30] E. Friedman, A. Gal and C.J. Batty, *Nucl. Phys.* **A579**, 518 (1994);  
C.J. Batty, E. Friedman and A. Gal, *Phys. Rep.* **287**, 385 (1997).
- [31] J. Schaffner, C.B. Dover, A. Gal, D.J. Millener, C. Greiner and H. Stöcker, *Ann. Phys. (N.Y.)* **235**, 35 (1994).
- [32] E. Friedman, A. Gal, J. Mareš and A. Cieplý, *Phys. Rev. C* **60**, 024314 (1999).
- [33] V. Koch, *Phys. Lett. B* **337**, 7 (1994).
- [34] T. Waas and W. Weise, *Nucl. Phys.* **A625**, 287 (1997).
- [35] G.Q. Li, C.-H. Lee and G.E. Brown, *Phys. Rev. Lett.* **79**, 5214 (1997); *Nucl. Phys.* **A625**, 372 (1997).

- [36] S. Pal, C.M. Ko, Z. Lin and B. Zhang, *Phy. Rev. C* **62**, 061903(R) (2000).
- [37] G. Baym, C.J. Pethick and P. Sutherland, *Astrophys. J.* **170**, 299 (1971).
- [38] J.W. Negele and D. Vautherin, *Nucl. Phys.* **A207**, 298 (1974).
- [39] C. Kettner, F. Weber, M.K. Weigel and N.K. Glendenning, *Phys. Rev. D* **51**, 1440 (1995).
- [40] J.M. Bardeen, K.S. Thorne and D.W. Meltzer, *Astrophys. J.* **145**, 505 (1966).
- [41] D.W. Meltzer and K.S. Thorne, *Astrophys. J.* **145**, 514 (1966).
- [42] Y. Sugahara and H. Toki, *Nucl. Phys.* **A579**, 557 (1994).
- [43] A.R. Bodmer, *Nucl. Phys.* **A526**, 703 (1991).

## TABLES

TABLE I. The nucleon-meson coupling constants in the GM1 set are taken from Ref. [24]. In this relativistic model, the baryons interact via nonlinear  $\sigma$ -meson and linear  $\omega$ -meson exchanges. The coupling constants are obtained by reproducing the nuclear matter properties of binding energy  $E/B = -16.3$  MeV, baryon density  $n_0 = 0.153$  fm $^{-3}$ , asymmetry energy coefficient  $a_{\text{asy}} = 32.5$  MeV, incompressibility  $K = 300$  MeV, and effective nucleon mass  $m_N^*/m_N = 0.70$ . The hadronic masses are  $m_N = 938$  MeV,  $m_\sigma = 550$  MeV,  $m_\omega = 783$  MeV, and  $m_\rho = 770$  MeV. The parameter set TM1 is obtained from Ref. [42] which incorporates nonlinear exchanges in both  $\sigma$  and  $\omega$  mesons. The nuclear matter properties in the TM1 set are  $E/B = -16.3$  MeV,  $n_0 = 0.145$  fm $^{-3}$ ,  $a_{\text{asy}} = 36.9$  MeV,  $K = 281$  MeV, and  $m_N^*/m_N = 0.634$ . All the hadronic masses in this model are same as GM1 except for  $\sigma$ -meson which is  $m_\sigma = 511.198$  MeV. All the parameters are dimensionless, except  $g_2$  which is in fm $^{-1}$ .

	$g_{\sigma N}$	$g_{\omega N}$	$g_{\rho N}$	$g_2$	$g_3$	$g_4$
GM1	9.5708	10.5964	8.1957	12.2817	-8.9780	—
TM1	10.0289	12.6139	4.6322	-7.2325	0.6183	71.3075

TABLE II. The coupling constants for antikaons ( $\bar{K}$ ) to  $\sigma$ -meson,  $g_{\sigma\bar{K}}$ , for various values of  $\bar{K}$  optical potential depths  $U_{\bar{K}}$  (in MeV) at the saturation density. The results are for the GM1 and TM1 set.

$U_{\bar{K}}$	-100	-120	-140	-160	-180
GM1	0.9542	1.6337	2.3142	2.9937	3.6742
TM1	0.2537	0.8384	1.4241	2.0098	2.5955

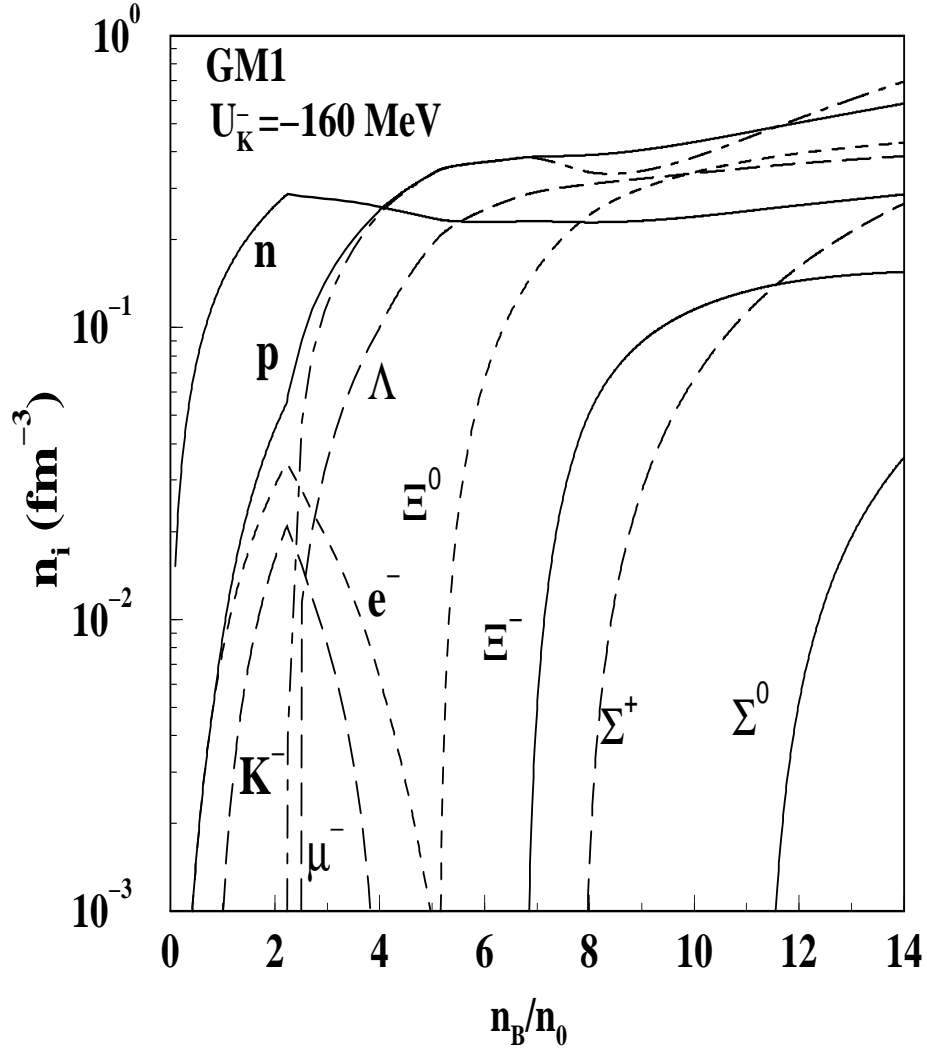


FIG. 1. The proper number densities  $n_i$  of various compositions in  $\beta$ -equilibrated hyperonic matter including  $K^-$  condensate for GM1 model and antikaon optical potential depth at normal nuclear matter density  $U_{\bar{K}} = -160$  MeV.

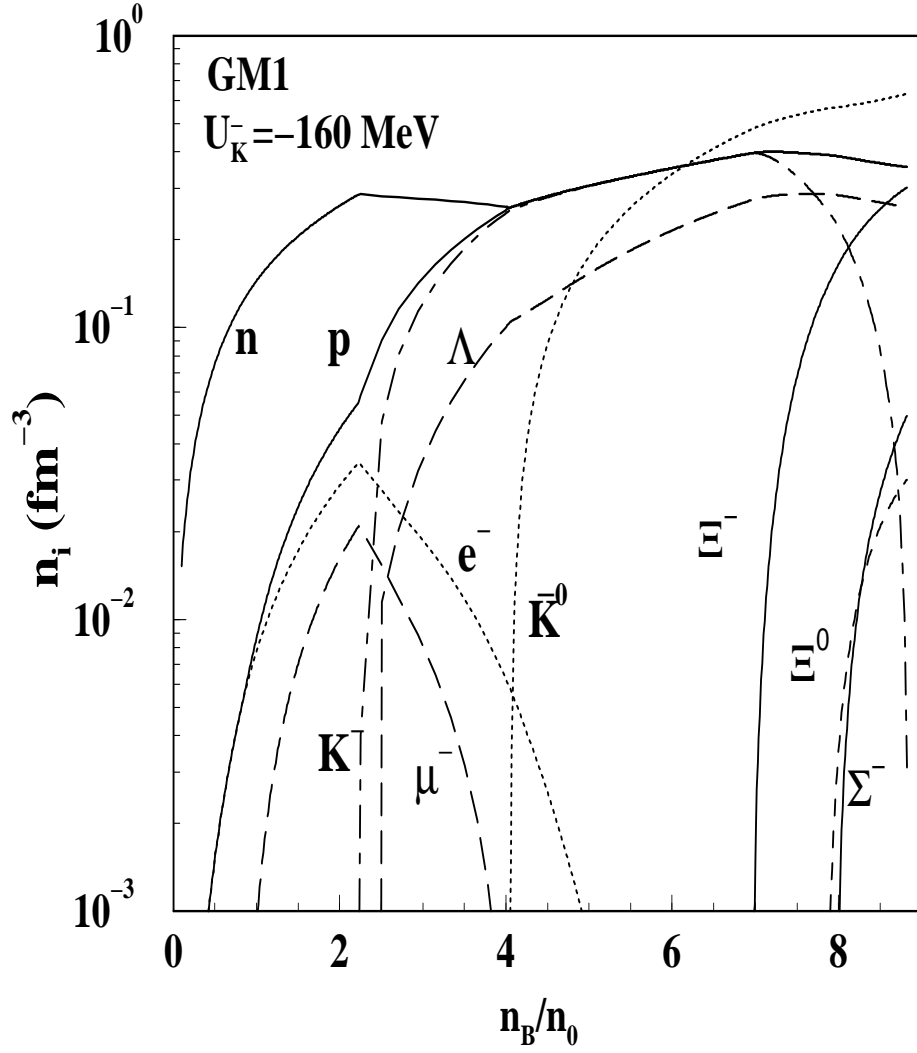


FIG. 2. The proper number densities  $n_i$  of various compositions in  $\beta$ -equilibrated hyperonic matter including both  $K^-$  and  $\bar{K}^0$  condensate for GM1 model and antikaon optical potential depth at normal nuclear matter density  $U_{\bar{K}} = -160 \text{ MeV}$ .

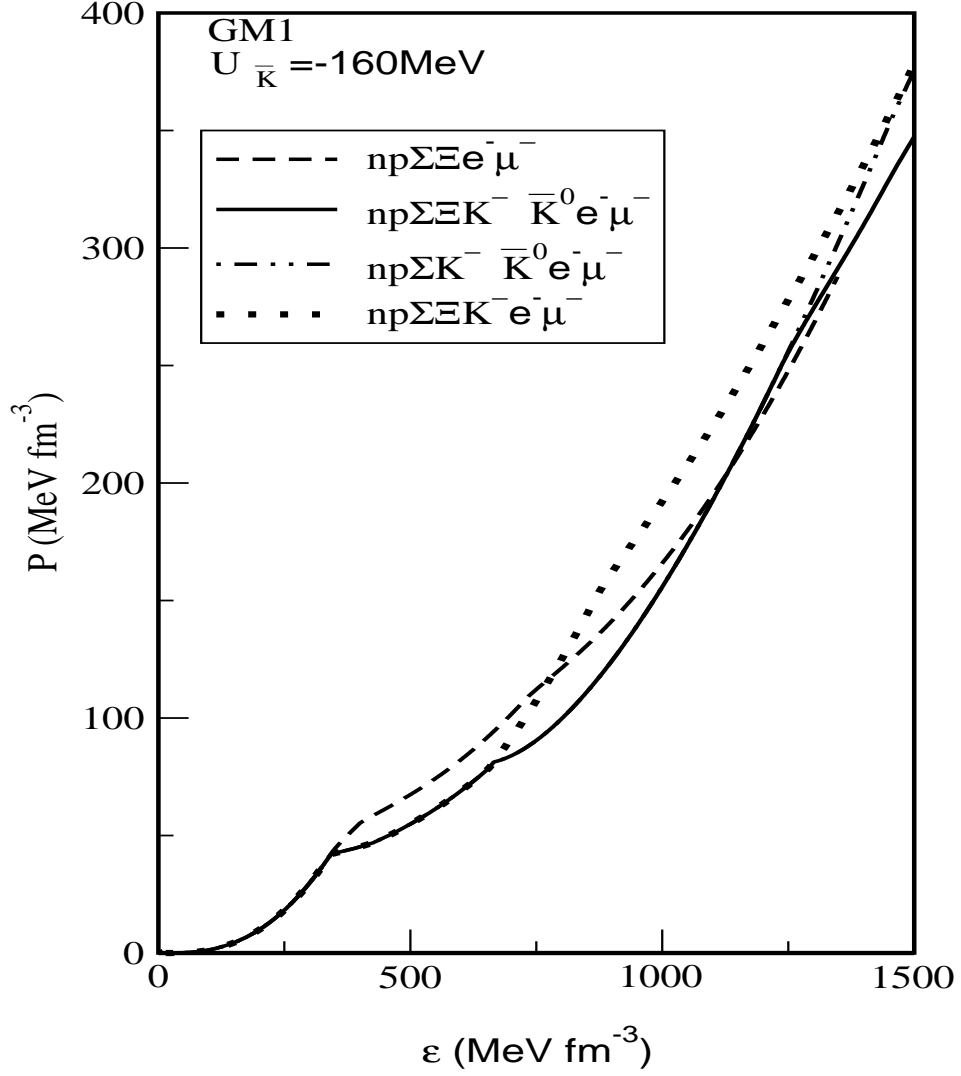


FIG. 3. The equation of state, pressure  $P$  vs. energy density  $\varepsilon$  in GM1 model. The results are for hyperonic matter (dashed line), hyperonic matter including  $K^-$  condensate (dotted line) and  $K^-$  and  $\bar{K}^0$  condensation in hyperonic matter (solid line) and in hyperonic matter excluding  $\Xi$  (dashed-dot line) calculated with the antikaon optical potential depth at normal nuclear matter density of  $U_{\bar{K}} = -160$  MeV.

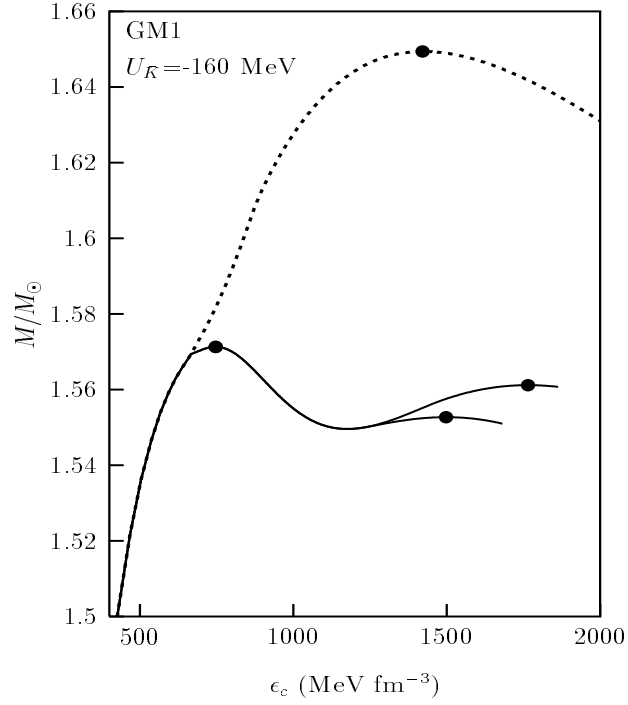


FIG. 4. The compact star mass sequences are plotted with central energy density for GM1 model and the antikaon optical potential depth of  $U_{\bar{K}} = -160$  MeV. The star masses of hyperonic matter with  $K^-$  condensate and with further inclusion of  $\bar{K}^0$  condensate are shown here. In the latter case, a second sequence of compact stars appears in the high energy density regime.

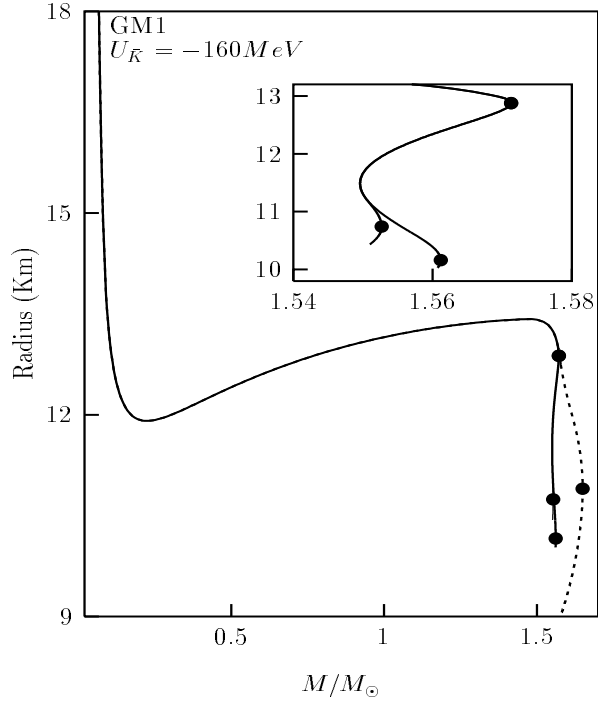


FIG. 5. The mass-radius relationship for compact star sequences for hyperonic matter with  $K^-$  condensate and with further inclusion of  $\bar{K}^0$  condensate for GM1 model and antikaon optical potential depth of  $U_{\bar{K}} = -160$  MeV. The mass-radius relationship for the third family branch is shown in the inset.